Joint Special Interest Group meeting between euspen and ASPE
Advancing Precision in Additive Manufacturing
Ecole Centrale de Nantes, France, September 2019
www.euspen.eu

Effect of measurement and sampling strategy in surface analysis of laser powder bed fusion additive manufacturing of nickel superalloy 625

Jason C. Fox[1], Adam Pintar[2]

[1]*Engineering Laboratory, National Institute of Standards and Technology*, USA*
[2]*Information Technology Laboratory, National Institute of Standards and Technology*, USA*

jason.fox@nist.gov

Abstract

As parts built through additive manufacturing (AM) increase in complexity, the development and understanding of appropriate methods to characterize the as-built surface will be required. In laser powder bed fusion (LPBF) AM, parts are built through a complex process with size scales that include single/sub-micrometer (e.g., cracks and fine topographic features on the part surface), tens of micrometers (e.g., feedstock powder diameters and layer thicknesses), hundreds of micrometers (e.g., laser scan hatch spacing and melt pool dimensions), single/tens of millimeters (e.g., laser scan stripe widths), and tens/hundreds of millimeters (e.g., part dimensions). This large range and complexity of the build process creates surfaces with complex topographies, large height ranges, and steep slopes when compared to machined surfaces and, therefore, uncertainty that a measurement sufficiently represents the full surface from which it was sampled. The goal of this work is to better understand the measurement and sampling strategy to aid development of measurement routines for AM parts. Currently, no recommendations exist for defining the required point spacing, size of measurement regions, or number of measurement regions required to adequately describe the as-built AM surface. In this work, a relatively large AM part is built in nickel superalloy 625 using a commercially available LPBF system to create a planar surface greater than 40 mm x 40 mm in size. The height data from the large surface area was subdivided into regions similar in size to single and stitched field of view (FoV) measurements to assess variation in areal surface parameters across the surface and their ability to statistically represent the entire surface. The result of this work provides an important step in developing guidance for the measurement of as-built AM surfaces.

additive manufacturing; laser powder bed fusion; measurement strategy; surface topography

1. Introduction

Additive manufacturing (AM) has emerged as a key technology for production of high-value and complex parts that reduces time-to-market and cost to manufacture [1]. Laser powder bed fusion (LPBF) in particular has generated a great deal of interest due to the fine detail in finished parts compared to other AM technologies [2]. A limitation hindering the widespread adoption of AM, however, is the as-built surface topography or, more specifically, a lack of understanding the relationships between the as-built AM surface topography and functional performance of the part.

This lack of understanding stems partially from the complex nature of the build process, but also from inadequate knowledge in the AM research community of appropriate methods for characterization of AM surfaces. While standards from ASME [3] and ISO [4], as well as an extensive library of "Good Practice Guides" from the National Physical Laboratory [5], exist to guide the evaluation of surface topography, little guidance exists in how to appropriately measure and characterize AM surfaces.

The research community is currently developing correlations of part function to surface texture, such as Gockel *et al.* [6]; however, without a strong understanding of the required fidelity, point spacing, measurement size, etc., it can be difficult to determine the quality of the correlation. Research, such as Fox *et al.* [7], Zanini *et al.* [8], and Thompson *et al.* [9], is actively addressing the issues of measurement fidelity and uncertainty, but there is still no direct guidance as to the method and requirements of an AM surface topography measurement.

The purpose of this research is to investigate the effect measurement and sampling strategy have on calculated parameters, as well as the ability to adequately represent a large surface measurement with a smaller set of sampled regions. To that end, a sample made from nickel superalloy 625 (IN625) with a large (over 40mm x 40 mm) planar surface was measured in a focus variation (FV) system with multiple focusing objectives. The data from these surface measurements are subdivided into common measurement sample sizes based on various numbers of stitched field-of-views (FoVs) and analyzed to determine the ability of the sample(s) to statistically represent the entire surface.

2. Methodology

The part used in this analysis was built on the EOS M290 system at the National Institute of Standards and Technology (NIST). The part, shown in Figure 1, was fabricated using

*Certain commercial entities, equipment, or materials may be identified in this document to describe an experimental procedure or concept adequately. Such identification is not intended to imply recommendation or endorsement by the National Institute of Standards and Technology, nor is it intended to imply that the entities, materials, or equipment are necessarily the best available for the purpose.

commercially available EOS NickelAlloy IN625 (corresponds to classification unified numbering system (UNS) N06625 [10]) using the vendor recommended parameter settings. It should be noted that the material used for the build was powder reclaimed from prior builds using an 80 µm sieve. It is assumed that the condition of the powder may have an effect on the surface topography of parts being built, and analysis of the powder is currently underway.

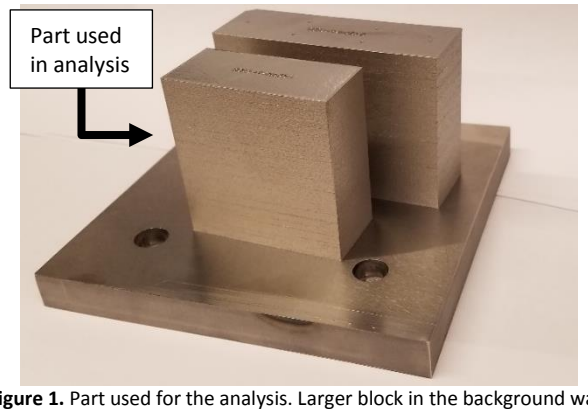

Figure 1. Part used for the analysis. Larger block in the background was not used in this analysis. Dimensions of the substrate are 12.7 cm x 12.7 cm x 1.3 cm.

Height measurements were taken from the vertical surface of the part (the surface perpendicular to the substrate) using an Alicona G5 InfiniteFocus system, which conforms to ISO 25178-606:2015 [11]. A 10x objective and 20x objective were used in the analysis, along with coaxial and ring (i.e., off-axis) lighting that was optimized for each scan. The Alicona's sensor pulls data in as an 1840 pixel by 1840 pixel grid for a single FoV and point spacings for measurements were approximately 0.88 µm and 0.44 µm for the 10x and 20x objectives, respectively. Thus, a single FoV measures (1.62 x 1.62) mm for the 10x objective and (0.81 x 0.81) mm for the 20x objective. To cover a large portion of the surface, stitched measurements of (31 x 31) FoVs and (60 x 60) FoVs for the 10x and 20x objectives, respectively, were performed. This created greater than 40 mm x 40 mm measurement regions at the previously mentioned point spacings. Measurements were taken at a minimum of 5 mm away from any edge of the part to minimize the effect of the part geometry on the surface texture. Three separate measurements were taken one after another for each objective and heights for each (x,y) location were averaged to reduce the effect of measurement noise.

Due to the large size of the measurement, the data could only be exported from Alicona's measurement software as a 16-bit depth image (this is the highest resolution option for export). In this export method, heights are converted to gray levels based on the full range of heights in the image. This led to a rounding of the vertical resolution to approximately 3.7 nm and 3.4 nm for the 10x and 20x objectives, respectively, which should have little influence on the result as this is lower than the stated height resolution of the equipment (50 nm for the 20x objective) [12]. Once exported as a depth image, the data was imported into MATLAB, averaged to reduce noise, and subdivided into smaller measurement samples. To replicate common sizes of measurement regions, the height data was subdivided based on equivalent stitched FoVs, assuming a 10% overlap for the stitching. The associated measurement sample sizes are presented in Table 1.

Table 1. Lateral size of measurement samples after stitching.

Stitched FoVs	Lateral Size of Measurement Sample		
	Pixels	10x obj. (mm)	20x obj. (mm)
1x1	1840	1.62	0.81
2x2	3496	3.08	1.53
3x3	5152	4.54	2.26
4x4	6808	5.99	2.98
5x5	8464	7.45	3.71
6x6	10120	8.91	4.44
8x8	13432	11.82	5.89

Using the sizes presented in Table 1, the large measurement region was subdivided into smaller measurement samples. The number of samples at each given size are presented in Table 2. Note that only whole measurement samples were pulled from the full area measurement and measurement samples did not overlap one another. Samples were centered in the full area of the measurement and excess data around the perimeter was neglected from the analysis. For example, for the 10x objective with a 2x2 FoV size, 13.68 x 13.68 samples can fit in the full measurement area, but only 13 x 13 samples, centered about the full measurement area, were pulled and the excess data around the perimeter is neglected.

Table 2. Number of measurement samples after subdividing the full area measured. Numbers marked as N/a were not used in this analysis either for brevity or due to memory limitation of the analysis computer.

Stitched FoVs	10x Objective		20x Objective	
	Count in x, y	Total	Count in x, y	Total
1x1	26	676	52	2704
2x2	13	169	27	729
3x3	9	81	N/a	N/a
4x4	7	49	17	289
5x5	5	25	N/a	N/a
6x6	N/a	N/a	9	81
8x8	N/a	N/a	7	49

Once data was subdivided it was exported from MATLAB, converted to the X3P format [13], and imported into the commercially available ConfoMap software for analysis [14]. To prepare data prior to calculation of parameters, the ConfoMap software was used to level the data, perform outlier removal using an 87° slope filter (this is the stated limitation of the Alicona system [12]), and filter the data with a Gaussian filter using nesting indices of S-filter = 2.5 µm and L-filter = 800 µm [15]. Parameters were calculated according to ISO 25187-2:2012 [4]. The remainder of the paper will focus on the root mean square height of the scale limited surface (*Sq*) for brevity, but results generally hold for other parameters as well.

3. Experiment Results

Example data from the 10x and 20x objective, Figure 2 and Figure 3, show that the data qualitatively agree. In general, there is more data dropout around the edges of the partially melted powder particles and scattered across the melt surface in the 10x data. This is expected as the 10x objective should have more difficulty with steep slopes at the edge of the spherical particles and with the finer topographic features due to the increased point spacing and different numeric apertures.

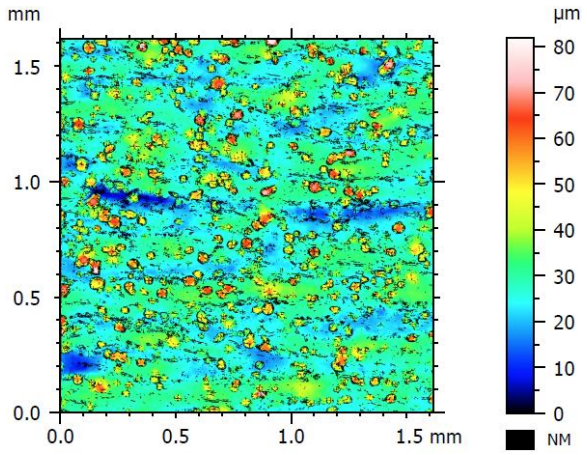

Figure 2. Height map from the 10x objective data subdivided to a single (1 x 1) FoV, where NM represents non-measured points.

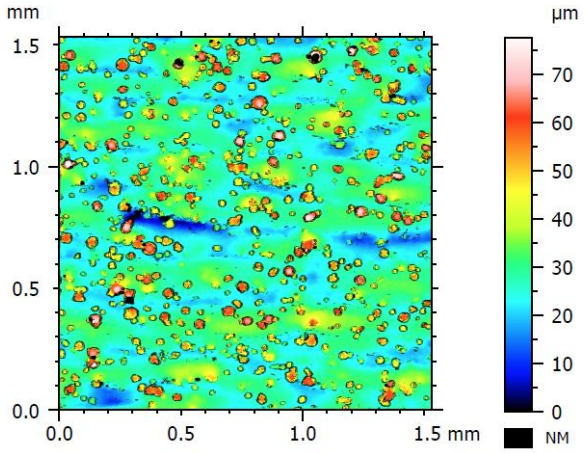

Figure 3. Height map for the 20x objective data subdivided to a (2 x 2) FoV, where NM represents non-measured points. A (2 x 2) FoV area is shown since the lateral size of the sample better compares to the 10x single FoV from Figure 2.

Additionally, surface texture parameters were calculated from the subdivided data and plotted based on the data's (x,y) position on the surface, shown in Figure 4 and Figure 5. From these figures there is little difference in the point-by-point calculation of parameters, values range from approximately 6.5 µm to 9.5 µm, and there appears to be spatial structure.

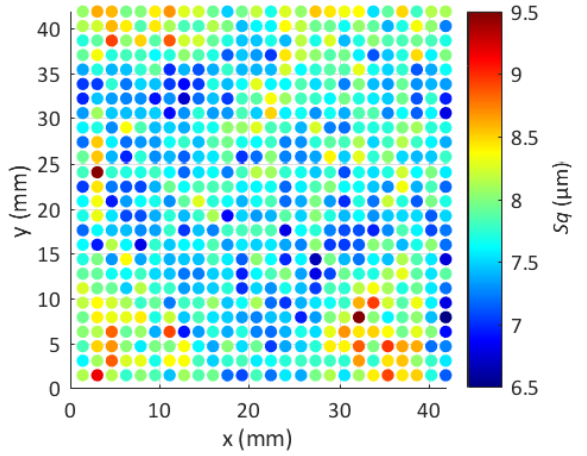

Figure 4. Calculated *Sq* for each single (1 x 1) FoV subset on the surface.

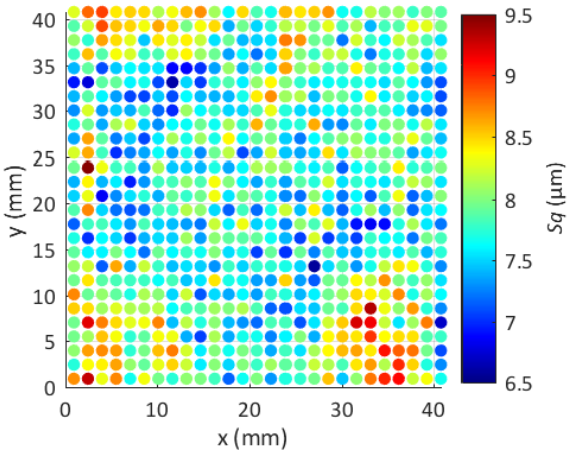

Figure 5. Calculated *Sq* for each (2 x 2) stitched FoV subset on the surface. A (2 x 2) FoV area is shown since the lateral size of the sample better compares to the 10x single FoV from Figure 4.

4. Discussion

As researchers are looking to relate surface texture parameters, such as *Sq*, to functional properties of the part, it is important to investigate the quality of the measurement process and the effect that may have on the results. Using the data presented in Section 3, an analysis of the average *Sq* values and associated standard deviation for each measurement sample size is shown in Figure 6. This figure shows that there is little statistical difference between the 10x objective and 20x objective in terms of average *Sq*. Additionally, there is a slight decrease in the standard deviation for both objectives as the lateral size of the sample increases. This is expected because, mathematically, as the size of the samples increases such that it approaches the size of the full measurement area (i.e., there is only one measurement sample covering the entire surface), the standard deviation should decrease to zero.

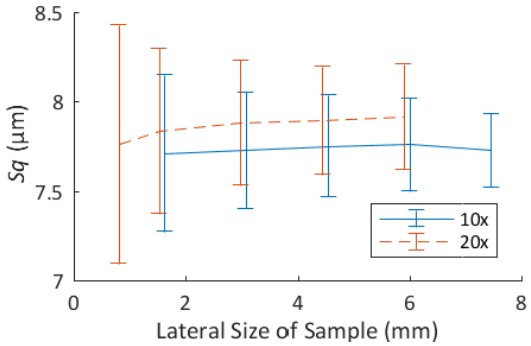

Figure 6. Average *Sq* and standard deviation for the 10x and 20x objective data versus lateral size of the measurement sample.

Since, however, it is not common to measure an entire surface, especially a large one, but rather to sample the surface across smaller regions, it is important to also examine the effect of that sampling on the measurement result. Figure 7, shows normalized histograms of *Sq* values for the different measurement sizes. On the left of the figure are the distributions of contiguous sampling (i.e., adjacent, stitched FoVs), where the top distribution is single FoVs and the bottom distribution is from a 5 x 5 FoV (25 total) stitched measurement. The distributions on the right are from averaging the same number of individual FoVs, selected at random and not necessarily adjacent, for 1000 iterations. For example, for the bottom right (i.e., Random Sampling with 25 FoVs), 25 random FoV measurements are taken from the single FoV data (i.e., the data shown in Figure 4). Those 25 *Sq* values are averaged and that process is repeated for 1000 iterations to make up the histogram

in the bottom right of Figure 7. From this data, it is evident that when using contiguous sampling, there is a limited improvement in the distribution beyond (3 x 3) FoVs (i.e., 9 stitched FoVs). In contrast, sampling randomly over space leads to histograms that are more nearly Gaussian, and continue to narrow in width as you increase the number of FoVs.

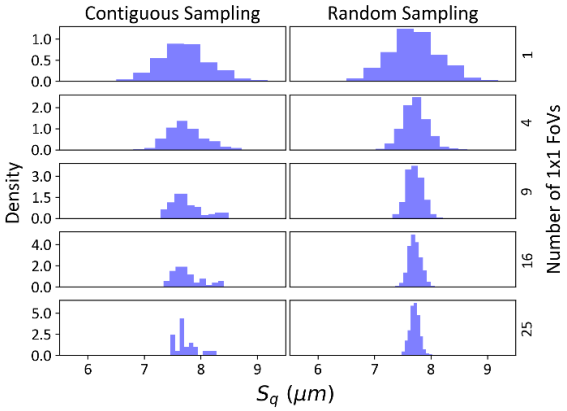

Figure 7. Histograms comparing contiguous sampling (i.e., stitched FoV) and random sampling for the 10x objective data.

Investigating the standard deviation of the *Sq* values, shown in Figure 8, the random sampling's standard deviation decreases at the rate of $\approx (1/\sqrt{n})$, where n is the number of selected samples. This decrease is much faster than for the contiguous sampling with stitched FoVs. We attribute this to the existence of spatial structure in the roughness measurements. That is, FoVs that are near one another tend to have a similar surface roughness (i.e., values of *Sq* in this case). Thus, even when a large contiguous area is measured, the measurement may not be representative of the whole part. In contrast, sampling randomly in space avoids this pitfall and provides a better characterization of the whole part.

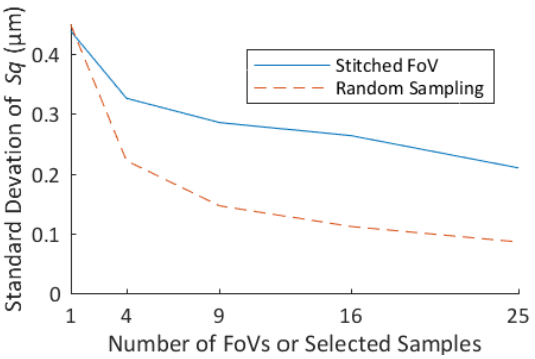

Figure 8. Comparison of the standard deviation of *Sq* for the contiguous sampling vs. random sampling.

5. Conclusions and Future Work

In this work, a large surface area measurement (over 40 mm x 40 mm) was performed on an IN625 part built through LPBF AM to determine the effect measurement and sampling strategy have on the ability to adequately represent such a large surface. Little difference was seen in the calculated parameters between the 10x and 20x objective even though differences in measurement fidelity are expected between the two. It is assumed that the 20x objective is a higher fidelity, but this cannot be confirmed without a calibrated AM surface measurement, which supports the importance of that field of research.

Results also show that the standard deviation of *Sq* decreases with increasing FoVs and the greatest decrease is between one and four FoVs for both stitched (2 x 2) and random sampling, which could be important in weighing measurement time versus accuracy. Based on the data presented, it is important to stress that the size of the measurement sample should be dictated by maximum spatial wavelength of the features the user is searching for [15]. This will allow the user to spread multiple samples across the surface, even at random, and thus gaining a stronger representation of the surface than the same number of FoVs in a contiguous, stitched measurement. While only data for *Sq* is shown in the paper, the relationships shown also hold for other common parameters (outside of extreme value parameters, such as *Sz* or *Sv*).

Future work on this topic will include rescaling to determine if results hold when approaching point spacings commonly seen in x-ray computed tomography surface analyses (greater than 1 µm point spacing), alignment of data for point-by-point deviation to better understand the difference between 10x and 20x data, and analysis of longer spatial wavelengths contained in the full area measurement of the part.

References

[1] Measurement Science Roadmap for Metal-Based Additive Manufacturing. Gaithersburg, MD: NIST, US Department of Commerce; 2012.

[2] Yadroitsev I. Selective laser melting: direct manufacturing of 3D-objects by selective laser melting of metal powders. Saarbrücken: Lambert Acad. Publ; 2009.

[3] ASME B46.1: Surface Texture (Surface Roughness, Waviness, and Lay), New York, NY 2009.

[4] ISO 25178-2:2012. Geometrical Product Specifications (GPS) - Surface Texture: Areal - Part 2: Terms, definitions, and surface texture parameters, ISO, Geneva. 2012.

[5] Petzing J, Coupland J, Leach RK. The Measurement of Rough Surface Topography using Coherence Scanning Interferometry. National Physical Laboratory Good Practice Guide No. 116, Teddington, UK: 2010.

[6] Gockel J, Sheridan L, Koerper B, Whip B. The influence of additive manufacturing processing parameters on surface roughness and fatigue life. *International Journal of Fatigue* 2019;**124**:380–8. doi:10.1016/j.ijfatigue.2019.03.025.

[7] Fox JC, Kim FH, Reese ZC, Evans C. Investigation of complementary use of optical metrology and x-ray computed tomography for surface finish in laser powder bed fusion additive manufacturing. *Proceedings of the euspen and ASPE SIG on Dimensional Accuracy and Surface Finish in Additive Manufacturing*, Leuven, Belgium: 2017, p. 132–6.

[8] Zanini F, Sbettega E, Sorgato M, Carmignato S. New Approach for Verifying the Accuracy of X-ray Computed Tomography Measurements of Surface Topographies in Additively Manufactured Metal Parts. *J Nondestruct Eval* 2018;**38**:12. doi:10.1007/s10921-018-0547-4.

[9] Thompson A, Senin N, Giusca C, Leach R. Topography of selectively laser melted surfaces: A comparison of different measurement methods. *CIRP Annals - Manufacturing Technology* 2017. doi:10.1016/j.cirp.2017.04.075.

[10] Material Data Sheet - EOS NickelAlloy IN625 2011. http://ip-saas-eos-cms.s3.amazonaws.com/public/d1327facdca0e32a/373a60ec4f5c891b7dbcdf572e37d3b0/EOS_NickelAlloy_IN625_en.pdf (accessed June 13, 2017).

[11] ISO 25178-606:2015. Geometrical product specification (GPS) -- Surface texture: Areal -- Part 606: Nominal characteristics of non-contact (focus variation) instruments 2015.

[12] Alicona. Technical Specifications of the Alicona InfiniteFocus. Alicona Focus Variation n.d.;English Edition 6.

[13] The OpenFMC repository for C/C++ and other code for reading and writing X3P files.: OpenFMC/x3p 2018. https://github.com/OpenFMC/x3p (accessed September 26, 2018).

[14] ConfoMap. Besançon, France: Digital Surf; 2018.

[15] ISO 25178-3:2012. Geometrical Product Specifications (GPS) - Surface Texture: Areal - Part 3: Specification operators, ISO, Geneva. 2012.